

A failure model for non-proportional loading under plane stress condition based on GFLC in comparison to eMMFC and PEPS

H Hippke¹ and B Berisha² and P Hora¹

¹Institute of Virtual Manufacturing, ETH Zurich, Tannenstrasse 3, 8092 Zurich, Switzerland

²inspire AG, inspire-ivp, Tannenstrasse 3, 8092 Zurich, Switzerland

hhippke@ethz.ch

Abstract. A mathematical model is presented for a forming limit for non-proportional loading under plane stress condition. The model results in an approach to reduce the number of experiments needed for the Generalized Forming Limit Concept (GFLC) and presents a numerical approach to calculate the linearized FLC from real Nakajima measurements. The mathematical model has been analyzed in comparison to Polar Effective Plastic Strain (PEPS) diagram and enhanced Modified Maximum Force Criterion (eMMFC), discussing both consistency with plasticity modeling and industrial applicability. An experimental setup based on Nakajima specimens is presented and DIC measurements are used to capture loading paths. The measured loading paths are used to validate predictions made by PEPS, eMMFC and the presented mathematical approach. The latter model shows promising results for prediction of failure for non-proportional loading.

1. Introduction

Correct prediction of localization failure in sheet metal forming is well established with the use of the forming limit curve (FLC) for proportional loading. Within the field of FLC determination, the three major influences discussed are non-proportional loading, curvature and pressure effects. Min et al. [1] presented an extended model to compensate for these effects which was applied to Marciniak [2] test and both large and small Nakajima test. The presented model however remains within the framework of GFLC, and focuses on non-proportional loading. The effect of non-proportional loading has first been shown by Nakajima et al. [3], with ongoing research presented by Stoughton and Yoon [4], Yoshida et al. [5] and Zhu et al. [6]. Failure prediction for non-proportional loading remains a field of extensive international research with a variety of models presented and industrially applied. This publication aims to contribute to the ongoing research by proposing an approach to reduce experimental effort within the framework of the GFLC model. To be able to evaluate the model, its performance is compared to two other established approaches, eMMFC and PEPS.

2. Derivation of analytical model

The modeling approach presented is based on damage accumulation along the path of failure up to the point of localization. A damage accumulation parameter λ is introduced as by Volk and Suh [7], which is equal to one at the point of localization. The variable accumulated is a ratio of incremental effective



plastic strain to a reference function, representing the limit of effective plastic strain in dependency of the incremental strain ratio β for ideally linear loading paths. The ratio β can be determined either directly as a function of the measured strain increments or in dependency of an arbitrary, convex yield locus function Φ as seen in Equation (1).

$$\beta = \frac{\Delta\epsilon_2}{\Delta\epsilon_1} = \frac{\partial\Phi(\sigma_1, \sigma_2)/\partial\sigma_2}{\partial\Phi(\sigma_1, \sigma_2)/\partial\sigma_1} \quad (1)$$

Additionally, two common auxiliary functions are introduced. The variable f represents the ratio of first principal stress to equivalent stress as a function of the yield locus as proposed by Volk and Suh [7] as $f(\alpha) = 1/\Phi(1, \alpha)$ and the variable $g(\beta) = (1 + \alpha\beta)f = \Delta\epsilon_v/\Delta\epsilon_1$ as derived from work equivalence in Hora et al. [8]. Despite the difference that the GFLC accumulates the lengths l_i , the two models are identical under plane stress assumption. This is shown in equation (2) using the definitions of β and $g(\beta)$.

$$\lambda = \sum \frac{\Delta l_i}{l_{flc}(\beta_i)} = \sum \frac{\sqrt{\Delta\epsilon_1^2 + \Delta\epsilon_2^2}}{\sqrt{\epsilon_{1flc}^2 + \epsilon_{2flc}^2}} = \sum \frac{\Delta\epsilon_1 \sqrt{1 + \beta_i^2}}{\epsilon_{1flc}(\beta_i) \sqrt{1 + \beta_i^2}} = \sum \frac{\Delta\epsilon_1}{\epsilon_{1flc}(\beta_i)} = \sum \frac{g(\beta_i) \Delta\epsilon_1}{g(\beta_i) \epsilon_{1flc}(\beta_i)} = \sum \frac{\Delta\epsilon_{vi}}{\epsilon_{vflc}(\beta_i)} \quad (2)$$

The GFLC model continues from this general approach by taking the measured FLC without prestrain as reference curve. By definition, this returns $\lambda = 1$ when the reference curve is reached on a linear path. However this reference curve is not sufficient for non-proportional loading paths, as $\lambda < 1$ is discovered at failure along bilinear paths. To adjust λ to be equal to one at the instance of localization, FLCs are measured for different preloading amount and direction and bilinear interpolation is used to return an estimate for any combination not experimentally tested. The resulting metamodel has been verified and has found industrial application.

The adjustment taken in this publication aims at a reduction of FLC measurements by changing one basic assumption: the basic Nakajima experiment for FLC evaluation does not yield an entirely linear loading path. In fact, all loading paths in Nakajima testing follow a biaxial loading direction prior to the designated loading direction and all Nakajima paths turn towards plane strain loading prior to localized necking as later discussed in Figure 2 (a). We now aim to take advantage of the known non-linearity intrinsic to Nakajima testing to return a reference FLC for truly linear paths by defining the sought after linear FLC as the objective of a mathematical optimization. The information needed to extract the reference FLC are the loading paths of the Nakajima specimen and their respective point of localization. To be able to formulate an optimization problem, it is most effective to define the forming limit ϵ_{vflc} as a function of β . In this publication a polynomial of 4th order is chosen, the coefficients of which are adjusted in the optimization. It lies within the nature of mathematical optimization that any function may be chosen that is able to represent the desired FLC shape. The polynomial approach is an example of one possible approach. The parameters λ_i represent the accumulated damage parameter for each strain path used in the optimization and λ is a vector thereof.

$$\min_{\mathbf{x}} E(\mathbf{x}) = \frac{1}{2} \|\lambda(\mathbf{x}, \beta) - 1\|^2, \quad \mathbf{x} = [a, b, c, d, e] \quad (3)$$

$$\lambda_i = \sum \frac{\Delta\epsilon_{vi}}{\epsilon_{vflc}(\mathbf{x}, \beta_i)}, \quad \epsilon_{vflc}(\mathbf{x}, \beta_i) = a\beta^4 + b\beta^3 + c\beta^2 + d\beta + e$$

As starting points, the coefficients of a fit of the standard FLC are used. For mathematical convenience, this fit occurs in β - ϵ_v space. The optimizer is a nonlinear least-square solver. No boundary constraints are set and a trust-region-reflective solver is used. The largest resulting error $E(\mathbf{x})$ is 1.55E-4.

Under the assumption, that the inherent non-linearity in Nakajima testing is enough to represent general cases of non-linear loading conditions, the resulting FLC may be used for arbitrary loading paths as a reference FLC.

Table 1. Material parameters for 4xxx-alloy aluminium. YLD2000 and Gosh hardening.

α_1	α_2	α_3	α_4	α_5	α_6	α_7	α_8	a
0.9285	0.9718	0.7253	0.9919	0.9766	0.7847	0.9414	1.2365	8
A [MPa]	B [-]	n [-]	C [MPa]	$\sigma_{y_{Gosh}} = A(B + \epsilon_v)^n - C$				
713.96	0.0052	0.0635	444.12					

3. Example of FLC evaluation

To be able to discuss the validity of the model, it is applied to a standard 4xxx-aluminum alloy without strain rate dependency. The material behavior is described using a YLD2000 type yield locus as introduced by Barlat and Yoon [9] with the parameters given in Table 1. While it is not used in the model presented, the yield curve parameters of a Gosh type approximation are given as well. These will be used for comparison with the eMMFC model as proposed by Hora and Tong [10] and studied by Manopulo et al. [11]. Both yield curve and yield locus are displayed in Figure 1 (a) and (b) respectively. The material tested has a thickness of 1 mm.

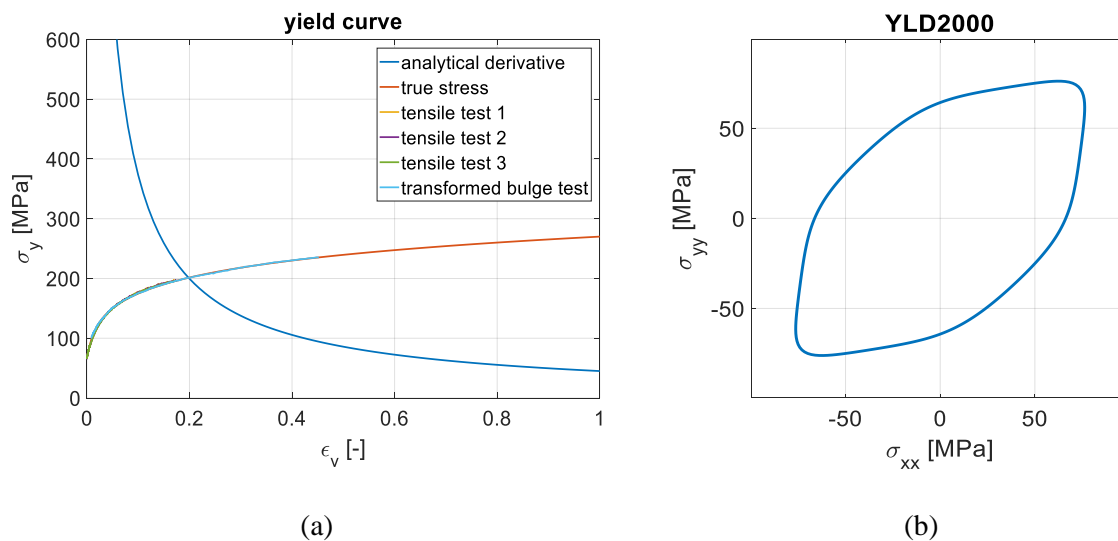


Figure 1. Yield curve (a) and yield locus (b) of the alloy used in all experiments.

For the determination of the linear FLC, three strain paths for the Nakajima configurations of standard widths B20, B50, B80, B90, B100, B120 and B200 were obtained and are used in the optimization process. Figure 2 (b) shows the respective loading paths in a $\beta - \epsilon_v$ space as introduced by Zeng et al. [12], this space is chosen precisely for its emphasis on path changes. It represents an alternative to the widely used triaxiality based $\eta - \epsilon_v$ representation space. Figure 2 (a) also includes the FLC based on the cross-section method according to ISO12004 [13] in major strain space and the back-transformation of the optimized linear FLC for reader convenience. Both curves are identically displayed in $\beta - \epsilon_v$ space, where optimization has taken place. We discover, that the minimum of the FLC has significantly moved towards the perfect plane strain state ($\beta=0$ or $\epsilon_2=0$). From first observation, we conclude that the optimization has returned a reasonable result, as the minimum occurs in plane strain state. The abrupt changes to the paths in $\beta - \epsilon_v$ space are due to the fact that β is the ratio of incremental major strains. Consequently, the major strains rotate if $\Delta\epsilon_2 > \Delta\epsilon_1$.

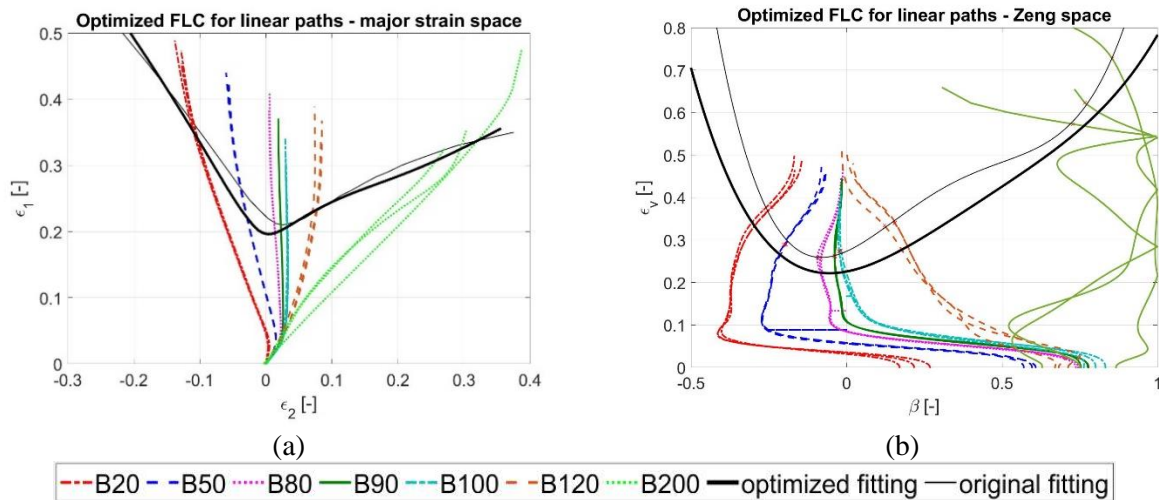


Figure 2. Measured strain paths of Nakajima specimen used in optimization. First in major strain space (a) and additionally in β - ϵ_v space (b). Both Figures show both the measured and the optimized FLC.

4. Comparison to first experimental results

Bilinear strain paths were measured for both 10% and 15% prestrain in tensile direction followed by a reduced set of Mini-Nakajima specimen in B200, B100 and B50 configuration as shown in Figure 3. These experiments are identical to Nakajima experiments scaled by a factor of 0.5, with the longer side equal to 100mm. For thin sheet material, the plane stress assumption remains valid, making Mini-Nakajima experiments more cost-effective. Additionally, since the model is designed to predict arbitrary paths, it is unnecessary to remain within the bounds of standard experiments. As long as the full deformation path is captured, any deformation that leads to localization is valid. Figure 4 shows the measured nonlinear paths in β - ϵ_v space with the measured failure position of the experiments marked in red and that of the proposed model in blue. The model clearly shows the correct tendencies, however, the result is conservative, as failure is predicted prior to the measured failure position. For reference the optimized FLC is shown in black.

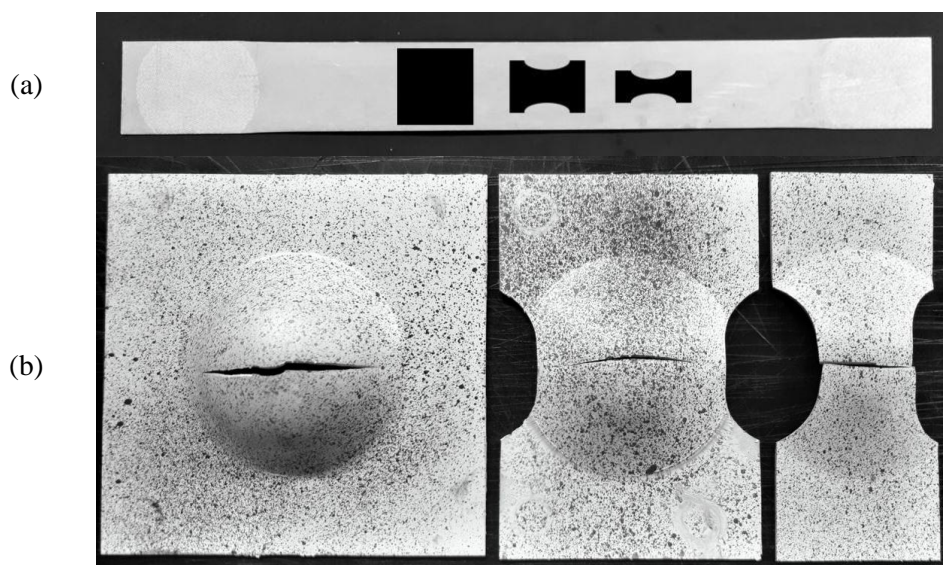


Figure 3. MiniNakajima experimental specimen for bilinear path evaluation (b) and tensile prestrain specimen (a).

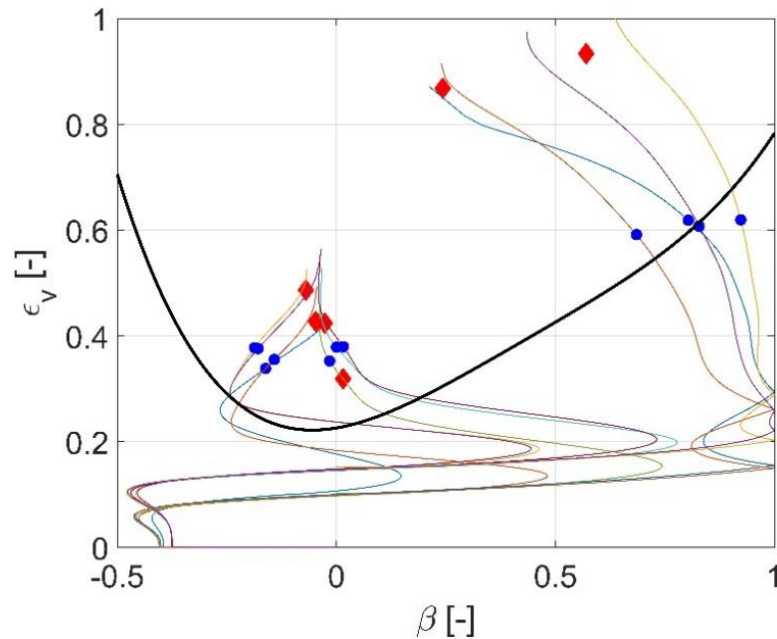


Figure 4. Measured nonlinear paths in β - ϵ_v space with measured (blue dots) and evaluated (red squares) failure points.

5. A comparative study

To put the results in perspective, a comparison with other models for nonlinear paths is drawn. Two additional models, eMMFC by Hora and Tong [10] and PEPS by Stoughton and Yoon [4] will be looked at in detail. For reader convenience, the eMMFC model for nonlinear paths and the PEPS model will be briefly summarized.

5.1. Enhanced Modified Maximum Force Criterion for non-proportional loading

The numerical implementation of the eMMFC criterion is defined incrementally and can be directly used for non-proportional loading paths. The general eMMFC criterion is given in equation (4), followed by its numerical form in equation (5) with H and H' representing the yield curve and its derivative. The reference curvature ρ_0 is implemented as discussed by Hora et al. [14] and is set to 25mm for Mini-Nakajima specimens, t represents the current thickness and t_0 is the initial thickness. To apply the eMMFC formulation to an arbitrary given loading path, the same algorithm may be used as for standard MMFC as introduced by Hora [8]. MMFC searches for the instance of localization along strictly linear paths until the maximum force criterion $dF \leq 0$ is met. To search for localization along arbitrary paths, the measured increments of β and ϵ_v are used to check the criterion. The material constants E_0 , and n are set to 0.1 and 0.6 respectively, as empirically determined by Hora and Tong [10]. For an arbitrary path given, the criterion is evaluated for each point along the path until the condition is met. The resulting points of localization are given in Figure 6 in direct comparison to PEPS and the new model.

$$\frac{\partial \sigma_1}{\partial \epsilon_1} \cdot \left[1 + \frac{t}{2\rho_0} + \frac{E_0}{2} \left(\frac{t}{t_0} \right)^n \right] + \frac{\partial \sigma_1}{\partial \beta} \frac{\partial \beta}{\partial \epsilon_1} \leq \sigma_1 \quad (4)$$

$$f(\alpha) H' g(\beta) \cdot \left[1 + \frac{t}{2\rho_0} + \frac{E_0}{2} \left(\frac{t}{t_0} \right)^n \right] \leq f(\alpha) H + \frac{f'(\alpha) g(\beta) \beta}{\beta(\alpha) \epsilon_v} H \quad (5)$$

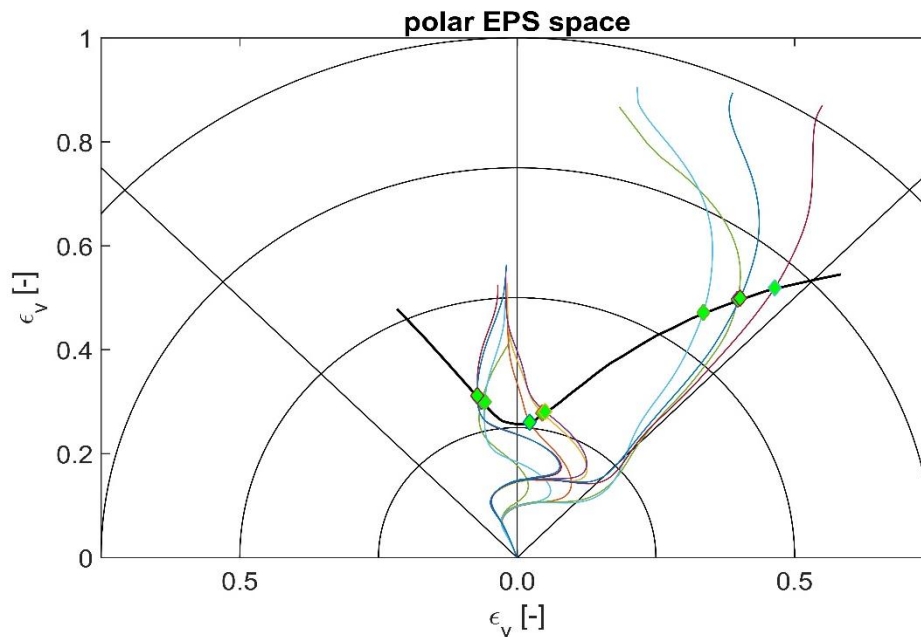


Figure 5. The loading paths in polar EPS space and indicates the points of failure at intersection with the measured FLC.

5.2. Polar strain diagram for failure evaluation

The polar strain diagram, as proposed by Stoughton and Yoon [4], suggests that in the space of angle θ and effective plastic strain ϵ_v , the same limit curve is valid for arbitrary paths. This is experimentally shown by transformation of a large number of measured strain paths by Stoughton and Yoon [4]. The angle θ is defined as $\theta = \arctan(\beta)$. Figure 5 shows the result in the polar space directly. However, to compare measurements, the position of failure along the path is also displayed in major strain space in Figure 6.

5.3. Discussion of comparative study

To evaluate the failure position along each strain path, the cross-section method was used. The surprisingly high strain values for the combination of tensile prestrain and biaxial second drawing remain under investigation. A possible explanation has been given by Min et al. [1] by studying the effect of contact pressure on both large and small Nakajima specimen. It is expected, that an extension of the model to include pressure effects will further improve the linearized FLC.

As presented in Figure 6, both eMMFC and PEPS show similar results for the majority of strain paths tested. The presented model shows good agreement with the measured failure for all except the biaxial cases, indicating that the model presented provides a valid approach to reduce the effect of non-proportional loading. The three models may be evaluated without a large number of experiments necessary, as they are based only on the Nakajima experiments done for standard FLC evaluation. In comparison to standard GFLC, this approach offers one possibility to reduce the amount of experiments.

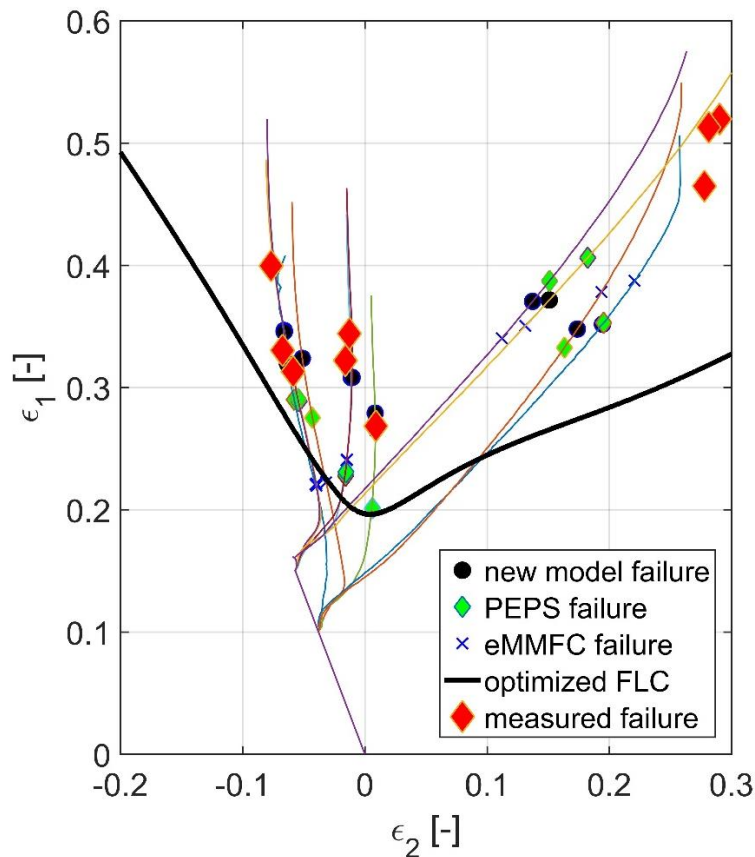


Figure 6. The failure prediction of all models discussed in FLD space.

6. Conclusion and outlook

The presented mathematical optimization using a 4th order polynomial as approximation for a linearized FLC is a first approach and initial testing of an additional model for determination of linearized FLCs. The model indicates the correct tendency to extract non-linearity from optically measured strain paths. As predominant contribution, an increase in measuring efficiency may be achieved by decreasing the number of necessary experiments in the framework of the GFLC. For a quantified analysis of robustness and precision of the model, further experiments are needed with different alloys and other sheet materials. Furthermore, effects of curvature and contact pressure will need to be taken into account. To be able to validate extended model approaches, standard and Mini-Nakajima experiments are planned for a number of materials to compare results and consequently adjust the current model.

References

- [1] J. Min, T. B. Stoughton, J. E. Carsley, and J. Lin, "Compensation for process-dependent effects in the determination of localized necking limits," *Int. J. Mech. Sci.*, vol. 117, pp. 115–34, 2016.
- [2] Z. Marciniak and K. Kuczyński, "The forming limit curve for bending processes," *Int. J. Mech. Sci.*, vol. 21, no. 10, pp. 609–21, 1979.
- [3] Nakazima K; Kikuma T; Hasuka K, "Study on the formability of steel sheets," *Yawata Tech Rep*, vol. 264, pp. 8517–30, 1968.
- [4] T. B. Stoughton and J. W. Yoon, "Path independent forming limits in strain and stress spaces," *Int. J. Solids Struct.*, vol. 49, no. 25, pp. 3616–25, 2012.
- [5] K. Yoshida, T. Kuwabara, and M. Kuroda, "Path-dependence of the forming limit stresses in a sheet metal," *Int. J. Plast.*, vol. 23, no. 3, pp. 361–84, 2007.
- [6] X. Zhu, L. Chappuis, and Z. C. Xia, "A path-independent forming limit criterion for stamping simulations," *AIP Conf. Proc.*, vol. 778 A, p. 459, 2005.
- [7] W. Volk and J. Suh, "Prediction of formability for non-linear deformation history using generalized forming limit concept (GFLC)," *AIP Conf. Proc.*, vol. 556, pp. 556–561, 2013.
- [8] P. Hora, L. Tong, and B. Berisha, "Modified maximum force criterion, a model for the theoretical prediction of forming limit curves," *Int. J. Mater. Form.*, vol. 6, no. 2, pp. 267–79, 2013.
- [9] F. Barlat *et al.*, "Plane stress yield function for aluminum alloy sheets - part 1: theory," *Int. J. Plast.*, vol. 19, no. 9, pp. 1297–319, 2003.
- [10] P. Hora and L. Tong, "Theoretical prediction of the influence of curvature and thickness on the enhanced modified maximum force criterion," *Numisheet*, no. October 2008, pp. 205–10, 2008.
- [11] N. Manopulo, P. Hora, P. Peters, M. Gorji, and F. Barlat, "An extended Modified Maximum Force Criterion for the prediction of localized necking under non-proportional loading," *Int. J. Plast.*, vol. 75, pp. 189–203, 2015.
- [12] D. Zeng, L. Chappuis, and Z. C. Xia, "A Path Independent Forming Limit Criterion for Sheet Metal Forming Simulations," *SAE Int. J. Mater. Manuf.*, vol. 1, no. 1, pp. 809–817, 2008.
- [13] ISO 12004-2, "Metallic Materials - Sheet and Strip - Determination of Forming Limit Curves - Part 2: Determination of Forming Limit Curves in the Laboratory," vol. 2, no. 40, 2008.
- [14] P. Hora, L. Tong, M. Gorji, N. Manopulo, and B. Berisha, "Significance of the local sheet curvature in the prediction of sheet metal forming limits by necking instabilities and cracks," *MATEC Web Conf.*, 2016.